Journal of Scientific & Industrial Research
Vol. 83, February 2024, pp. 204-213
DOI: 10.56042/jsir.v83i2.5588

Control Strategy for LVRT Enhancement in Photovoltaic Fuel Cell Hybrid Renewable Energy System

Devvrat Tyagi[1], Ayushi Prakash[2], Amita Pal[3], Sonu Kumar Jha[4], Mayur Rahul[5] & Vikash Yadav[6]*

[1]National Institute of Electronics and Information Technology, Delhi, India

[2]Ajay Kumar Garg Engineering College, Ghaziabad, Uttar Pradesh, India

[3]Marathwada Mitra Mandal's Institute of Technology, Pune, India

[4]Galgotias University, Greater Noida, Uttar Pradesh, India

[5]UIET, CSJM University, Kanpur, Uttar Pradesh, India

[6]Government Polytechnic Bighapur Unnao, Department of Technical Education, Uttar Pradesh, India

Received 14 September 2023; revised 01 January 2024; accepted 17 January 2024

The present work describes a Low voltage ride through (LVRT) method for optimizing a photovoltaic fuel cell hybrid renewable energy system (HRES). The LVRT control approaches were previously studied to apply them to systems such as Wind Power Generation (WPG) and Solar Energy Generation (SEG), among other things. Photovoltaic (PV) power generation systems have recently drawn significant interest, with the building of large PV systems or groupings of systems related to the utility grid gaining a lot of traction. As a result of the significant penetration of photovoltaic electricity into the system, energy regulatory bodies enact increasingly strict grid rules to preserve grid stability. This paper demonstrates a large-scale grid-connected solar system along with the associated modeling and control approaches that can be utilized to improve DC-based voltage levels which can ride-through capabilities of solar power plants. The grid side inverter is essential for low-voltage driving. In case of overvoltage or under voltage the grid may trip inverter's DC link thereby such variation should be avoided as much as feasible. The purpose of this research is to incorporate DC-link over and under-voltage protection into the control loop without raising the cost of the protective device, which is a significant consideration. In the future, a study of the outcomes using a typical inverter system is also planned. Numerous fault scenarios with increasing severity are analyzed to show that the comprehensive control system is effective. The most recent grid code for the distributed generation system is considered.

Keywords: DC-link, Dynamic voltage recovery, Energy generation, Energy storage system, Grid stability

Introduction

Photovoltaic systems, according to the International Energy Agency, will be one of the most significant sustainable powers near plans. Globally, expensive photovoltaic systems continue to decline as the average selling price of components continues to fall. According to statistics from the Photovoltaic 2014 market guide, globally, Photovoltaic systems deployments achieved 136.7 GW at the end of 2013, and a total market increase has gained 36% over the last five years. Environmental concerns, renewable energy, a rise in gasoline prices, political obstacles, and the cost of systems all contribute to the high penetration of systems into electrical networks. Additionally, rather than taking years, the MW photovoltaic power plants are constructed in a matter of months.[1]

Large-scale solar power facilities have been linked to the primary grid in recent years. Numerous challenges occur due to this extensive integration only with the electricity network, such as the evolution of these systems' Low Voltage Ride Through (LVRT) capability. As solar energy has become more prevalent in electric networks, grid provision and maintenance have become more significant for wireless carriers. Solar photovoltaic systems were recently issued distribution transformer grid codes by utilities, requiring plans to generate and assist grid disturbances. Numerous ways have been utilized to understand better, evaluate, and improve the LVRT capabilities of photovoltaic systems.[2]

A concentrated control method was planned to show the LVRT ability of single-stage matrix associated photovoltaic frameworks that included controlling both the genuine and responsive force streaming out of the photovoltaic framework. The

*Author for Correspondence
E-mail: vikas.yadav.cs@gmail.com

authors' study was expanded to include the use of the same control technique to non-transformer photovoltaic systems.[3] It was initially brought up regarding the effect of PV systems' dynamic performance on short-term voltage stability. Controlling the grid-side inverter has been proposed using an inverter controller with cascaded Proportional-Integral (PI) control. Furthermore, the PI controller has been employed in several studies to modify the LVRT of generator systems. Despite its reliability and applicability in many industrial applications, the PI controller is sensitive to parameter fluctuations and nonlinearity in dynamic systems.[4]

In recent years, several optimization algorithms have been used to solve the problem, with varying degrees of success. Energy generation from renewable sources is the most viable choice to satisfy the constantly growing energy needs and reduce environmental damage.[5] Installing wind turbines in places with sufficient wind has proven to be the most efficient renewable energy source in generating significant electric power. Since it creates no greenhouse gases or air pollution and uses little water, wind energy is the most environmentally friendly energy.[6] Wind energy has seen a dramatic surge in popularity due to lower initial investment costs and the advanced technology used to manufacture high-power wind turbines.[7] According to the definition, power quality is the amount of electricity sufficient for the equipment to perform correctly. Low-quality power can be identified by voltage fluctuations, sag/swell, and other symptoms of poor power quality. Listed below are a few of the technical ramifications of wretched powerfulness quality. Unreliable power quality can lead to system failure. This means that wind turbines must be equipped with LVRT (low-voltage ride-through) capacities to maintain grid connectivity in the event of a severe voltage decrease.[8]

It's essential to note that for the turbine protection system to accurately calculate the voltage sag (Vx) and fault clearance time (Tx), it first needs to detect the defect's location, kind of fault, and severity. Four can be used to summarize the required break move through the behavior of a wind farm, which is as follows:

i) However, a system failure lasting up to 140 milliseconds must not prevent the wind farm from being connected. Wind farms must maintain grid connectivity when the super grid voltage drops for more than 140 milliseconds.[9]
ii) Wind farms must provide the most primary frequency possible to the power grid during short circuits and volatility droops without surpassing the plant's quick rating.
iii) A wind farm must produce at least 90% of its pre-fault active power within 0.5 seconds of the problem being remedied for system defects lasting up to 140 milliseconds. There should be at least 90% of the wind farm's active power restored within a second of the voltage, reaching 90% nominal when a voltage dip lasts longer than 140 milliseconds.
iv) During voltage drops of much more than 140 milliseconds, a wind farm's operational power generation capacity must be maintained as minimum proportional to the adjusted power grid voltage.

Material & Methods

Photovoltaic System

Solar energy is converted into electricity via photovoltaic cell, a semiconductor diode. In practice, a PV module is made up of several PV cells. A single module or a series of concurrent combinations of several modules may be used depending on the application. A photovoltaic framework, frequently known as a PV framework or a sunlight based force framework is a force framework that produces usable sun based power utilizing photovoltaic.[10] It incorporates sun-powered chargers for retaining and changing over daylight into energy; a sun oriented inverter for changing the yield from direct to substituting flow, just as mounting, wiring, and another electrical frill for assembling the framework.

Solar cells are encased to protect them from the elements and ensure that the electrical connections are solid and corrosion-resistant. A module's typical construction is presented in Fig. 1. The cells are enclosed in an airtight shell made of the polymer

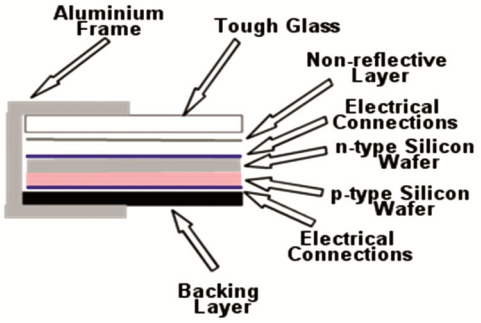

Fig. 1 — Module typical construction

Ethylene Vinyl Acetate (EVA), which cushions and protects them during shipping and handling due to their fragility. To ensure that the maximum quantity of light reaches the cell, the top cover is constructed of tempered glass with an anti-reflection coating.[11] The phone is shielded from substance assault by a covering of polyvinyl fluoride (F), regularly known as Tedlar, a manufactured polymer $(CH_2CHF)_n$ that goes about as a dampness hindrance. To make mounting and handling more accessible and provide additional protection, an aluminium frame is used. For aesthetic reasons, frameless modules are occasionally utilized in facades. This industry standard is employed since the photovoltaic module must "survive" outside for at least 20–25 years in various weather conditions, including some that are extreme. BECAUSE OF THIS DESIGN, the modules will last at least a lifetime.[12] Panel manufacturers, for example, guarantee 85% of minimum guaranteed power output after 25 years of operation, 93% after 12 years, and five-year materials and quality warranty. Compared to most things, such an extended guarantee is exceptionally long due to the better design of modules.

LVRT

Grid resiliency and supply security are two essential components of energy supply. Power plants must have control capacities and assurance components to avoid control outages. Traditional power plants were previously entirely responsible for supplying these demands. Meanwhile, in the collective power period, the availability of sustainable power sources has shown to be critical, to the point where these sources should contribute disproportionately, rendering the lattice roundness impossible. As a result, transmission system administrators have devised fictitious lattice codes with particular fundamental values and control features that generating facilities must adhere to a significant element needs, which is the purported LVRT capacity of manufacturing operations.

LVRT is an acronym for low voltage ride-through, which expresses the necessity that manufacturing plants remain operational while connected to the network during brief times of low matrix voltage. Voltage drops (Fig. 2) can happen at any time, such as when the matrix is under excessive strain or due to lattice faults like lightning strikes or short circuits. Energy-generating facilities, such as turbines aerated, were previously permissible to detach from the network in the instance of a malfunction and reconnect after a predetermined length of time.[13] Given the large offer of renewable today, such an approach would be fatal. A "power outage" occurs when many producing plants fail simultaneously, causing the entire system to fall. As a result, the LVRT requirement was to ensure that developing plants remained connected to the matrix. Furthermore, specific matrix codes require the network to be strengthened during voltage drops. Producing plants can help to reinforce the lattice by keeping the system's receptive current flowing and thus boosting the voltage. After allowing for blame leeway, the dynamic power yield must be adjusted to an incentive before the occurrence of blame within a set time frame. Photovoltaic frameworks and, more recently, Combined Heat and Power (CHP) facilities must now meet these requirements, which were previously only linked with wind turbines.[14]

Energy Storage System-based Method to Enhance LVRT Capability

Energy Storage Systems (ESSs) are currently used in various situations. Super Capacitive Storage System (SCSS) and Battery Energy Storage System (BESS) are two ESSs used in wind energy generating. Several FACTS devices are also available to help enhance the LVRT of wind electricity. On the other hand, hybrid systems are more cost-effective and efficient in terms of operation than a single ESS because each ESS is bound by its own set of limitations.[15] In BESS, frequent battery charging and discharging has a considerable impact on battery life.[16,17] As a result, a third energy source should be added to the WT system to improve its dependability. Various research methodologies suggested many micro-grid topologies that rely on renewable energy.[18–20] A simultaneous compensator gives the imperative responsive force while a breeze turbine generator gives the necessary dynamic power.[21]

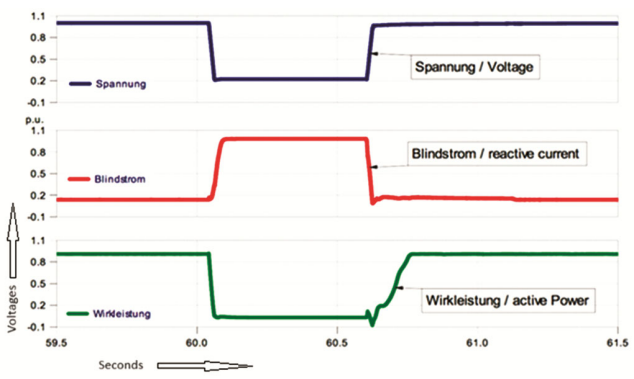

Fig. 2 — Example of the results of a voltage drop test

Hybrid Energy Storage System

The article examines the benefits of joining a super capacitor into a battery stockpiling framework for a DFIG-based breeze creation framework. At the place of traditional association, the SCSS and BESS are associated with Power Change Frameworks (PCSs) that should administer bidirectional force streams (PCC). For this situation, Energy executives Calculation (EMA) have been created to arrange the activity of the battery stockpiling framework and the super capacitor.[22] The schematic design in Fig. 3 illustrates how HESS is integrated with the Wind System to help stabilize power fluctuations. Additionally, when the storage is charged (i.e. Pb >0 and Ps >0), positive numbers and vice versa represent their powers.

LVRT Control Technique for Solar Photovoltaic Systems

The WPG System's LVRT Control Strategy

The WPG system setup, which utilizes a side adaptor, is shown in Fig. 4. In this framework, which likewise contains a side connector (with a unique breaker), an inverter, and a three-stage matrix, the generator is associated with a sharp edge. The side

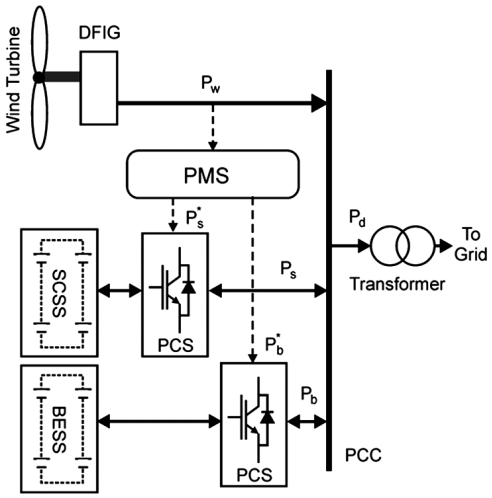

Fig. 3 — Integration of wind energy conversion system in the hybrid energy storage system

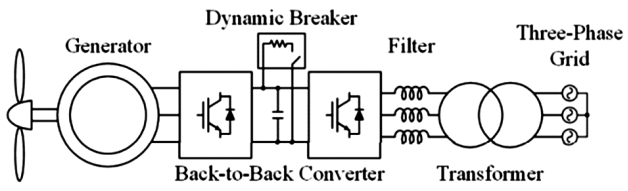

Fig. 4 — The wind power system setup using a back-to-back converter

inverters design is the most often used topology in WPG systems. It consists of a wind turbine inverter, a Switch with a flexible breakpoint, and a power system converter, among other elements. Because of the reduced grid voltage, the power limited by the rating current in the WPG system's power limiter mechanism is reduced during low grid voltage times.

As a result, there is extra power, which raises the voltage across the DC-link substantially. On the other side, a change in blade speed or DC-link voltage might cause the WPG system to malfunction and eventually fail. As a result, when the grid's voltage falls below a certain level, the WPG system's LVRT control mechanisms should be devised to keep the WPG system running smoothly. The WPG system demands the employment of a second device to consume excess power, assure LVRT compliance, and stay stable operations.[23]

The side converter includes a dynamic breaker, sometimes known as a crowbar. The crowbar is comprised of a resistor and a switch. The amount of reactive current (I_{de}) required to meet the LVRT requirement is determined by the LVRT control mechanisms for the WPG system operating at low grid voltage. Additionally, it estimates the active current (Ice) required to transfer the active power permitted within the current rating range of the WPG system (Rating).

$$I_{qe} = \sqrt{I^2{}_{rating} - I^2{}_{de}} \quad \ldots (1)$$

The quantities Ide and Ice, which signify the responsive and dynamic forces, separately, indicate the simultaneous reference casing's d-q hub flows. These concerns are taken into account when the grid-side inverter is controlled. The dynamic breaker kicks in to bring down the voltage across the DC-link when the blade is rotating at its maximum speed.[24]

Additionally, reactive current must be injected during voltage drops to aid in fault clearing and grid voltage recuperation. Wind turbines should stay associated with the network and give receptive force when the PCC voltage dips under the blue region[25] as indicated in Fig. 5.

The SEG System's LVRT Control Strategy

As shown in Fig. 6, single-stake geography without a DC/DC converter or two-stage DC/DC converter engineering systems may be built. This framework is contained a few parts, including photovoltaic clusters, a force transformation framework, A three-phase grid with a filter.

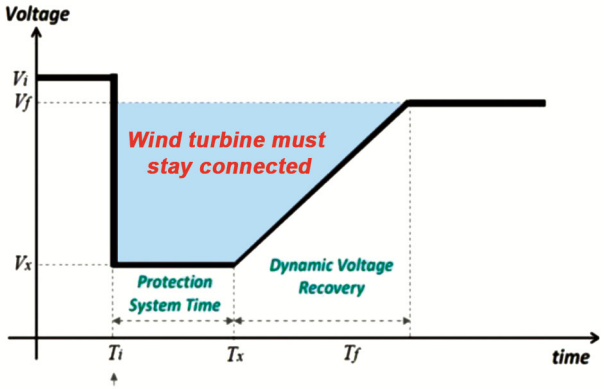

Fig. 5 — Variation of PCC dips voltage concerning time

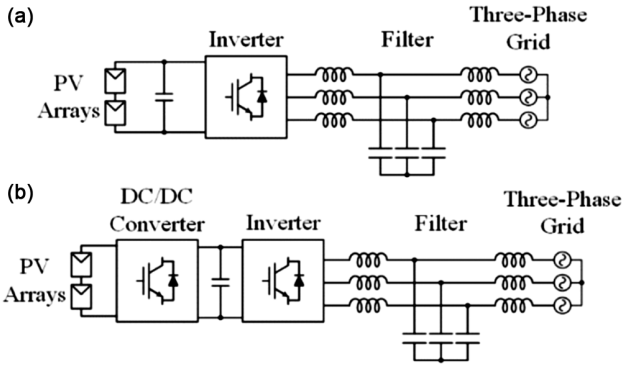

Fig. 6 — Solar energy generation system configurations: (a) Single-stage architecture without a DC/DC converter, and (b) Dual-stage architecture with a DC/DC converter

Responsive force is infused into the framework side inverter in the SEG framework if the lattice voltage dunks in the framework, paying little mind to geography, to meet the LVRT prerequisite, which is indistinguishable from that in the WPG framework. Then again, the LVRT control instruments utilized in SEG frameworks vary in a few different ways from those used in WPG frameworks. Since the LVRT control methodology with the most extreme force age is more effective, it is frequently utilized in the SEG framework. The d-pivot current (I_{de})which is significant for receptive force infusion into low-voltage frameworks is controlled by the degree of low voltage using a Low-Voltage Responsive Force Move (LVRT) control system. Moreover, the dynamic flow is determined to guarantee that the most significant measure of power is moved from the photovoltaic clusters to the matrix at a low voltage: Eq. (1).

In contrast with WPG frameworks, the LVRT control approach used in SEG frameworks is principally centered on power generation. Adjusting the information control of the DC/DC converter to the

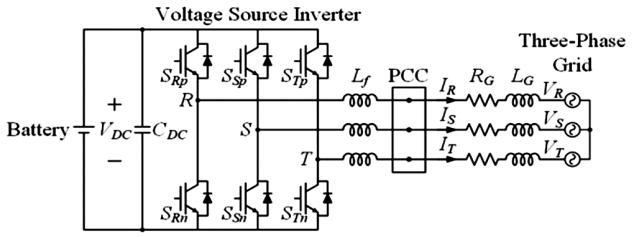

Fig. 7 — Circuit layouts of the Grid-connected energy storage system (ESS) (VSI)

Table 1 — Wind farm voltages tolerate limits

Voltage (KV)			
Nominal	% Limit of variation	Maximum	Minimum
400	+5% to −10%	420	360
220	+5% to −10%	245	200
132	+10% to −9%	145	120
110	+10% to −12.5%	121	96.25
66	+10% to −9%	72.5	60
33	+5% to −10%	34.65	29.7

specified power of output using I_{ge} and the low voltage grating is illustrated in Fig. 6(b).

The maximum and minimum voltage that withstands the limitations of wind farms operating at speeds above and below the rated speed value as depicted in Table 1.

Results and Discussion

Analysis of PCC Voltage Variation and Proposed ESSS Grid-Connected LVRT Control Strategy

The circuit setups of the ESS that is associated with the framework and fueled by a voltage source inverter are displayed in Fig. 7 (VSI). The framework has contained a battery, DC-connect capacitors (C_{DC}), a voltage stabilizer (VSI), a channel (L_f), resistive and inductive impedance (R_G) components on the network, and a three-stage power supply. The VSI contains six protected entryway bipolar semiconductors (IGBTS) associated in series with antiparallel diodes. The channel is associated with the three-stage network utilizing a PCC, or latent current authority. Its three-stage design produces consistently adjusted three-stage lattice voltages (V_R, V_S and V_T).

Recommendation for an LVRT Control Strategy Grid-Connected ESS

For the LVRT control technique to be effective, it must be used in a grid-connected ESS with a significant power scale. In some circumstances, this technique considers the peculiarities of the source type or the use of the framework overall. Notwithstanding its qualities or application, the

fundamental point of an LVR control technique is to fulfill the LVRT necessity and infuse receptive force into the lattice using a network side inverter, as characterized by matrix code prerequisites.

The grid-connected ESS differs from the WPG and SEG systems in that it supports bidirectional force stream dependent on charging and releasing conditions, while the WPG and SEG frameworks don't. Subsequently, when fostering an LVRT control system for a framework associated with ESS, it is essential to account for both charging and releasing circumstances.

Under discharging and charging conditions, ESS operation causes a drop in grid voltage. When this occurs, the proposed LVRT control method for matrix-associated ESS frameworks is like the procedures utilized for WPG and SEG frameworks. As per network code guidelines, the proposed LVRT control approach decides the measure of receptive current to infuse into the three-stage matrix to infuse responsive force into the three-stage network. Additionally, the active current used to transmit Active power within the rated current range of the ESS is determined when connected to the grid.

In Fig. 8, the supply voltage proportion of the multiple grids is plotted as a function of time to determine the amount of natural and reactive current to inject. The voltage-level computation procedure determines the multiple grid voltage levels (LEVEL) in a three-phase system by inputting the multiple grid voltages V_R, V_S and V_T. Because grid-code requirements necessitate LVRT, LEVEL is divided into three portions, each of which calculates total reactive current injection volumes differently. Under typical situations, if LEVEL is more significant than 90% of the multiple grid voltage, the overall resistant flow into the various grids is zero. In this circumstance, the reactive currently serves as the reference current, whereas the active wind is the reference current.[26] If V_{LEVEL}'s reactive current injected into the tri-phase network is more than 50% but less than 90% of the three-phase grid voltage. The reactive power injected into the multiple grids is equal to the draft of the networked ESS, and the active wind is zero for multiple Grid Voltages less than 50% of their respective three-phase grid voltages. Depending upon the V_{LEVEL} variations the multiple reactive current are derived based on the three phase grid's voltage drop ratio. The voltage variation leads to inject the maximum current in case of more than 90% level i.e. negligible resistance is observed.

The computations of the voltage level are represented by the V_R, V_S and V_T grid voltages as the inputs in Fig. 9. V_R (mag), V_S (mag) and V_T (mag) are used to calculate the magnitudes of each phase's voltage. The three-phase net voltages, such as the orthogonal signal generator (V_R (shift), V_S (change), and V_T (shift)) are computed using an all-pass filter. Here all-pass filter is utilized to generate estimated value of voltage level according to all three input voltages. LEVEL is calculated with the addition of the other variables utilizing the V_R (mag), V_S (mag) and V_T maximum value estimation method (mag). In the computation of the tension-level approach, the LEVEL-value obtained from the three-phase grid magnitude is essential. It is utilized to measure if

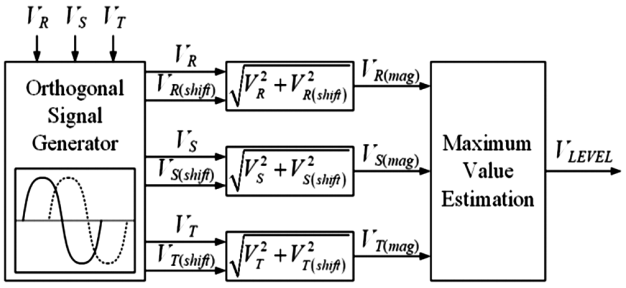

Fig. 9 — Calculation of voltage levels using three-phase grid voltages

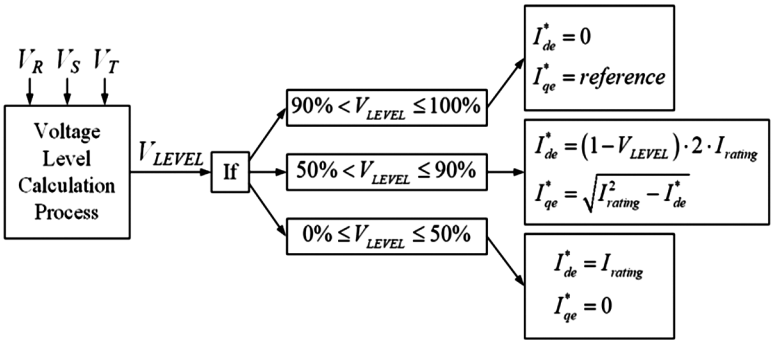

Fig. 8 — Calculation of the injection quantity of active and reactive currents based on the three-phase grid's voltage drop ratio

LVRT technology is needed. Consequently, the proposed LVRT control method calculates the injecting quantities of active and reactive currents based on the three-stage grid-regulated voltage drop ratio.

The grid-connected ESS control block schematic utilizing the proposed LVRT control technique is shown in Fig. 10. The phase-locked loop is used to get the Three-phase grid phase angle, and the V_R, V_S and V_T are used to do so (PLL). They're also used in the voltage-level computation technique, which is in charge of determining LEVEL. LEVEL and the LVRT control approach are used to determine the active and reactive reference currents, respectively.

Analysis of PCC Voltage Variation

While the ESS has the active current in the discharge state generated by the ESS is discharged into the three-phase grid.[27] As a result, the Reactive current phase injected into the grid of three stages affects the PCC voltages in this case. The PCC voltage varies according to the Reactive current phase when the ESS is discharged, as illustrated in Fig. 8.

V_G denotes grid voltage, while I_G denotes grid Current flow from the three-phase grid between the ESS. As this research shows, the ESS transmits energy to the three-phase grid when the I_G is positive. The d-axis represents the reactive component, whilst the active ingredient is represented by the q-axis.[28] In a three-phase grid, the PCC voltage (V_{PCC}) is equal to the sum of the resistor–voltage drops and inductor voltage drops (V_{RG} and V_{LG}). The active current (I_G) as shown in Fig. 11(a) imply a low reactive current. The V_{PCC} results in a phase similar to that of I_G due to the occurrence of V_G, V_{RG} and V_{LG}. When a three-phase grid is supplied with an inductive or capacitive reactive current, as shown in Fig. 11(b) and (c), the voltage potential varies due to the phase change of V_{RG} and V_{LG}, in other words injecting inductive reactive current decreases V_{PCC}, whereas injecting capacitive reactive current increases it, as illustrated in the graph. As a result, injecting active current and Capacitive reactive grid current improves V_{PCC} and meets the demand for low voltage reactive current (LVRT) under discharge situations.[29]

The suggested LVRT control method is essential to ensure that the ESS follows the LVRT, notably when the framework voltage decreases in an ESS connected to the network. The recommended LVRT control procedure builds up the measure of dynamic and receptive current infused into the three-stage matrix dependent on the voltage drop proportion of the three-stage lattice. Notwithstanding the ESS's functional qualities, for example, charging and releasing conditions, the infusion of capacitive receptive current builds the LVRT needed because of an increment in V_{PCC}. The suggested LVRT control strategy is validated by simulation and experimentation, and oscillations in the grid-connected ESS's PCC voltage are explored.

LVRT Control Strategy Dependent on the Battery's State of Charge

The battery charging state (SOC), in the DC-well field of the ESS associated with a DC source battery, should be considered, as illustrated in Fig. 4, for the LVRT control methodology for the ESS associated with a DC battery, as opposed to the LVRT control approach for WPG and SEG frames. The SOC is a vital indication used to govern operating decisions and prevent the battery system from overcharging or over-discharging. Sensors, on the other hand, cannot directly measure it. The battery management system or several techniques for predicting SOC based on the battery model are explained in detail below, are frequently used to determine SOC.[30–32] As previously stated, the suggested LVRT control mechanism can be applied when the SOC of a grid-connected ESS is greater or less than the authorized value for the ESS's

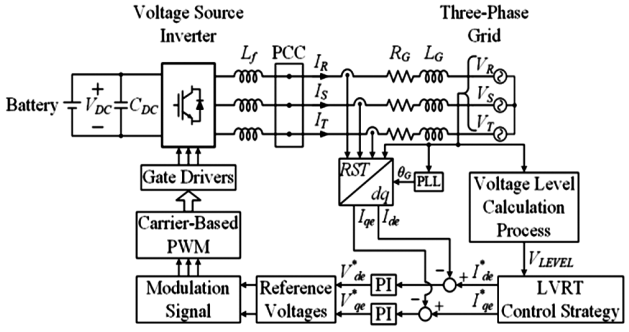

Fig. 10 — Diagram of the grid-connected control block with the suggested LVRT control approach

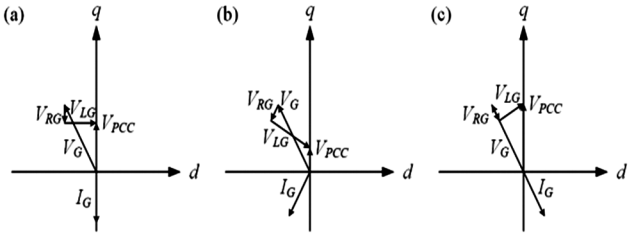

Fig. 11 — PCC voltage variations under the loading conditions of the ESS as a function of the reactive current's phase: (a) There is no reactive current, (b) an Inductive injected reactive current; and (c) A powerful reactive current is injected

discharging or charging conditions. However, if the SOC is less than or greater than the permitted value when the grid-connected ESS is discharging or charging the SOC should be considered when the grid-connected ESS's LVRT control plan is developed. This means that if the SOC of a grid-connected ESS falls below the authorized value during discharge conditions, the active current required by the three-phase grid cannot be provided. Thoughtless of whether the grid voltage decreases or rises, the reactive current is controlled by as rating current of the grid-connected ESS.[33] In overall the SOC variation is under compensation along with the suggested LVRT control mechanism i.e. rating current of the grid to be efficient control strategy.

Power Flow Distribution Control Strategy in HESS

At the start of each dispatching period, the SCSS power is calculated using the best ZLF and an optimized smoothing time constant. In this work, Fig. 12 depicts the proposed HESS power flow control allocation. The SCSS compensates for the quickly fluctuating wind power component (due to sudden changes in demand) and allows for the filtered power Pf for low variations. BESS power is then defined using an average filtered power dispatch method to supply the grid with a constant power Pd.

According to current PCS development, SCSS and BESS are successfully considered managing their power references (i.e. $P^*s = P_w - P^*_f$ and $P^*_b = P_f - P^*_d$). In contrast, the Power dispatch and wind power filtering are expected to match every reference.

Calculation of the SCSS Power Flow

The ZLF calculates the SCSS's power output because it considers rapidly varying wind power components. The filtered power variations with and without ZLF has been presented which indicates gap with respect to time. We developed an ideal ZLF to minimize time delay and decrease storage capacity. The ZLF specifies that the phase of the pass-band region shall be zero degrees, and the volume should be expressed in decibels (Db). In the meanwhile, the magnitudes of the top strip should be minimized. However wind power, filtered power, and SCSS power are determined using ZLF as shown in Fig. 13. Large variations are observed for SCSS's power P_s with ZLF. Because of wide application of bandwidth various energy storage systems are being used. Especially for generation of wind energy, SCSS

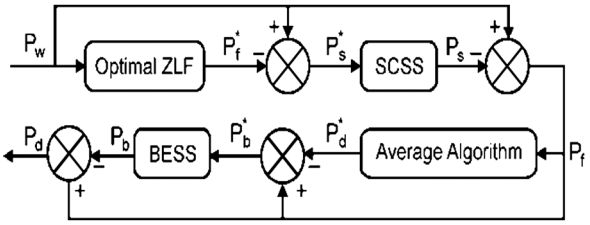

Fig. 12 — A proposed control method for the HESS's power allocation

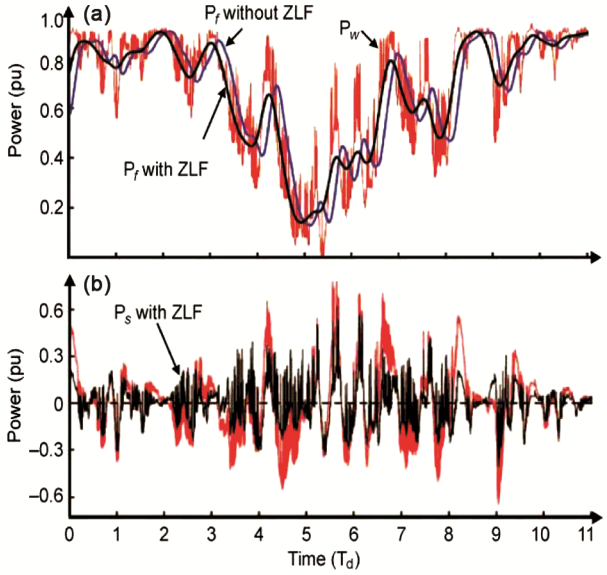

Fig. 13 — The power flow of the SCSS respecting the ZLF: (a) Wind power and the filtered power, and (b) SCSS power

and BESS are found to be very prominent. The durability of battery is dependent on charging and discharging processing. In case of SCSS, it is capable enough to compensate fluctuations for wind power. Experiments were performed using MATLAB simulation platform keeping turbine power ranging from 1.5 MW to 2 MW and wind speed 10 to 14 (m/s). As a result the performance of grid arrangement is found in line with the expectation of optimized control strategy.

Conclusions

This paper contributes towards a control methodology for improving LVRT in a half breed photovoltaic power device as per environmentally power framework. The proposed control approach has been utilized to coordinate both the network side inverter and the DC-DC converter to follow the most significant force point. The proposed LVRT control strategy is essential to ensure that the ESS follows the

LVRT, especially when the framework voltage decreases in an ESS connected to the network. The recommended LVRT control procedure builds up the measure of dynamic and receptive current infused into the three-stage matrix dependent on the voltage drop proportion of the three-stage lattice. The CMPN versatile separating method was used to powerfully refresh the PI regulator's relative and indispensable increases progressively. The reproduction results show that the framework reactions got utilizing the CMPN calculation based versatile control system is more damped and predominant than the Taguchi approach-based ideal PI control technique. The proposed versatile control procedure can be significantly further developing framework associated photovoltaic force plants' LVRT abilities. Further the proposed technique can be utilized to achieve a similar objective using various sustainable power frameworks.

References

1 Okundamiya M S, Size optimization of a hybrid photovoltaic/fuel cell grid connected power system including hydrogen storage, *Int J Hydrog Energy*, **46** (2021) 30539 – 30546.

2 Hassani H, Zaouche F, Rekioua D & Belaid S, Feasibility of a standalone photovoltaic/battery system with hydrogen production, *J Energy Storage*, **31** (2020) 101644.

3 Maleki A & Askarzadeh A, Comparative study of artificial intelligence techniques for sizing a hydrogen-based stand-alone photovoltaic/wind hybrid system, *Int J Hydrogen Energy*, **39** (2014) 9973–9984.

4 Azaroual M, Ouassaid M & Maaroufi M, Model predictive control-based energy management strategy for grid-connected residential photovoltaic–wind–battery system, in *Renewable Energy Systems*: *Modelling, Optimization and Control — A Volume in Advances in Nonlinear Dynamics and Chaos (ANDC)*, edited by A T Azar & N A Kamal, (Academic Press) 2021, 89–109, https://doi.org/10.1016/B978-0-12-820004-9.00014-0.

5 Ferahtia S, Djerioui A, Zeghlache S & Houari A, A hybrid power system based on fuel cell, photovoltaic source and supercapacitor, *SN Appl Sci*, **2**, 940 (2020).

6 Ogbonnaya C, Abeykoon C, Naseer A, Turan A & Ume C S, Prospects of Integrated Photovoltaic-Fuel Cell Systems in a Hydrogen Economy: A comprehensive review, *Energies*, **14** (2021) 6827.

7 Hoppmann J, Volland T S, Schmidt V H & Hoffmann, The economic viability of battery storage for residential solar photovoltaic systems - A review and a simulation model, *Renew Sustain Energy Rev*, **39** (2014) 1101–1118, doi:10.1016/j.rser.2014.07.068.

8 Tamalouzt N, Benyahia N, Rekioua T & Rekioua D, Wind Turbine DFIG/Photovoltaic/Fuel Cell Hybrid Power Sources System Associated with Hydrogen Storage Energy for Micro-grid Applications, *Int Renew Sustain Energy Conf Morocco*, **3** (2015) 10–13.

9 Kawabe & K Tanaka, Impact of the dynamic behaviour of photovoltaic power generation systems on short-term voltage stability, *IEEE Trans Power Syst*, **30** (2015) 3416–3424.

10 Elkalashy N I, Mosaad M I & Ashmawy M G, Integrating Adaptive Control of Renewable Distributed Switched Reluctance Generation and Feeder Protection Coordination, *Electric Power Syst Res J*, **154** (2018) 452–462.

11 Banakher F A, Mosaad M I, El-Rouf M O & Al-Ahmer L O, Maximum Power Point Tracking of PV system Based Cuckoo Search Algorithm; review and comparison, *Energy Proc*, **162** (2019) 117–126.

12 Mosaad M I, Alenany A, Siada A A & Elnaggar M, Application of Superconductors to Improve the Performance of DFIG-based WECS, *IEEE Access J*, **7** (2019) 103760–103769.

13 Mosaad M I, Alenany A & Siada A A, Enhancing the Performance of Wind Energy Conversion Systems using Unified Power Flow Controller, *IET Gen Trans*, (2020), doi.org/10.1049/ietgtd.2019.111

14 Agalar S & Kaplan Y A, Power quality improvement using STS and DVR in wind energy system, *Renew Energy*, **118** (2018) 1031–1040.

15 Hossain & Ali M H, Low voltage ride-through capability enhancement of grid-connected PV system by SDBR, *IEEE PES T&D Conf Expo*, **1** (2014) 1–5.

16 Ambia M N, Hasanien H M, Al-Durra A & Muyeen S M, Harmony search algorithm-based controller parameters optimization for a distributed-generation system, *IEEE Tran Power Del*, **30** (2015) 246–255.

17 El-Raouf M O A, Mosaad M I, Al-Ahmar M A, El Bendary F M, MPPT of the hybrid solar-wind-grid power generation system, *Int J Ind Electron Drive*, **2** (2015) 234–241.

18 Bendary A F & Ismail M M, Battery Charge Management for Hybrid /Wind/Fuel Cell with Storage Battery, *Enrgy Procedia*, **62** (2019) 107–116, https://doi.org/10.1016/j.egypro.2019.04.012.

19 El-Raouf M O A, Mosaad M I, Mallawany A, Al-Ahmar M A & Bendary F M E, Optimal Control of DVR to Enhance the Power Quality of /Wind/Fuel Cell Hybrid System Feeding a New Community, *Int Conf Electr Distribution*, **25** (2019) 599–603.

20 Maleki A, Rosen M & Pourfayaz F, Optimal Operation of a Grid-Connected Hybrid Renewable Energy System for Residential Applications, *Sustainability*, **9** (2017) 1314.

21 Ayadi O, Al-Assad R & Al-Asfar J, Techno-economic assessment of a grid-connected photovoltaic system for the University of Jordan, *Sustain Cities Soc*, **39** (2018) 93–98.

22 Samy M M, Alshammari N & Asumadu J, Optimal economic analysis study for renewable energy systems to electrify remote region in kingdom of Saudi Arabia, *IEEE Int Mid East Pow Sys Conf Egypt*, **25** (2018) 1040–1045.

23 Elmouatamid A, Ouladsine R, Bakhouya M, Kamoun M E, Khaider M & Zine-Dine K, Review of control and energy management approaches in micro-grid systems, *Energies*, **14** (2021) 168.

24 Photovoltaic Cell, Module, String, Array, Word Power-Ian Woofenden, 2006.

25 Yang Y, Blaabjerg F & Wang H, Low-voltage ride-through of single-phase transformerless photovoltaic inverters, *IEEE Trans Ind Applicant*, **50** (2014), 1942–1952.

26 Maleki A, Khajeh M G & Rosen M A, Two heuristic approaches for the optimization of grid-connected hybrid solar–hydrogen systems to supply residential thermal and electrical loads, *Sustain Cities Soc*, **34** (2017) 278–292.

27 Zhang G, Wu B, Maleki A & Zhang W, Simulated annealing chaotic search algorithm-based optimization of reverse osmosis hybrid desalination system driven by wind and solar energies, *Sol Energy*, **173** (2018) 964–975.

28 Barakat S, Samy M M, Eteiba M B & Whaba W I, Optimization of an off-grid /biomass hybrid system with different battery technologies, *Sustain Cities Soc J*, **40** (2018) 713–727.

29 Mosaad M I, Model reference adaptive control of STATCOM for grid-integration of wind energy systems, *IET Electr Power Applic J*, **12** (2018) 605–613.

30 Prajyusha A, Rao N S & Naresh B, Development of ultracapacitor-based DVR for power quality improvement, *Int J Innov Technol Res*, **6** (2018) 7822–7824.

31 Pal R & Gupta S, Recapitulation of various topologies and control strategies implicated in dynamic voltage restorer (DVR) for power quality improvement, *Int J Appl Eng Res*, **13** (2018) 3057–3073.

32 Praslin W J & Edward, J B, A review on impacts of power quality, control and optimization strategies of integration of renewable energy based microgrid operation, *Int J Intell Syst Appl*, **3** (2018) 67–81.

33 Ramadan H S & Mosaad M I, Power quality enhancement of grid connected fuel cell using evolutionary, *Comput Tech Int J Hydrogen*, **43** (2018) 11568–11582.